Science Advances
AAAS

Supplementary Materials for

Pathogen effector AvrSr35 triggers Sr35 resistosome assembly via a direct recognition mechanism

Yan-Bo Zhao *et al.*

Corresponding author: Songying Ouyang, ouyangsy@fjnu.edu.cn; Peiyi Wang, wangpy@sustech.edu.cn

Sci. Adv. **8**, eabq5108 (2022)
DOI: 10.1126/sciadv.abq5108

This PDF file includes:

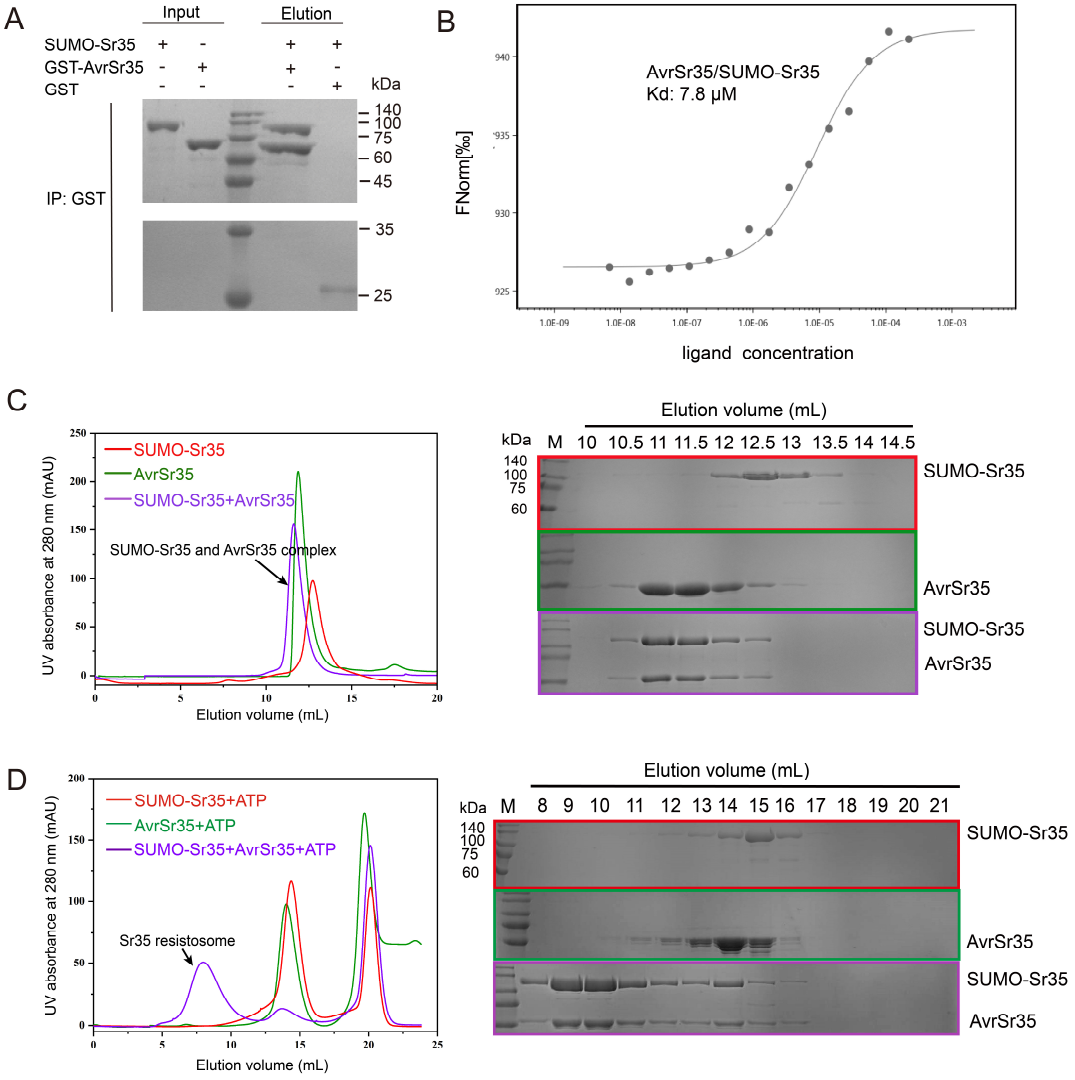

Fig. S1. Purification and reconstitution of Sr35-AvrSr35 complex and the Sr35 resistosome. (**A**) Sr35 interacts with AvrSr35 in GST pull down assay. GST-tagged AvrSr35 was incubated with SUMO-tagged Sr35, followed by affinity capture with glutathione resin. Eluted protein samples were analyzed using SDS-PAGE and Coomassie Blue staining. (**B**) Measurement of binding affinity between Sr35 and AvrSr35 with microscale thermophoresis (MST). The experiment was performed in binding buffer (25 mM HEPES (pH 7.5), 500 mM NaCl). The dissociation constant (Kd) of 7.8 μM is indicated above the binding curve. (**C**) Analysis of Sr35-AvrSr35 complex formation by gel filtration. SUMO-tagged Sr35 was incubated with AvrSr35 at 1:2 molar ratio at 4 °C for 2 h, after

which the mixture was analyzed using gel filtration column (Superdex 200, GE Healthcare). SUMO-tagged Sr35 and AvrSr35 samples were used as controls. Left panel: gel filtration profiles of SUMO-Sr35 (red), AvrSr35 (green), and the SUMO-Sr35-AvrSr35 complex (purple). Right panel: SDS-PAGE analysis of the peak fractions displayed in the left panel. The rectangles enclosing each gel are color-coded according to the left panel. Approximate corresponding elution volumes are displayed above the gels. (**D**) Oligomerization of Sr35-AvrSr35 complex in the presence of ATP. SUMO-Sr35 was mixed with AvrSr35 at 1:2 molar ratio in the presence of 1 mM ATP and incubated overnight at 4 °C, followed by analysis using gel filtration column (Superose 6, GE Healthcare). In the presence of ATP, the Sr35-AvrSr35 complex oligomerizes, whereas Sr35 or AvrSr35 alone do not. Left panel: gel filtration profiles of SUMO-tagged Sr35 (red), AvrSr35 (green) and SUMO-tagged Sr35-AvrSr35 complex (purple). SDS-PAGE analysis of the peak fractions displayed in the left panel. The rectangles enclosing each gel are color-coded according to the left panel. Approximate corresponding elution volumes are displayed above the gels.

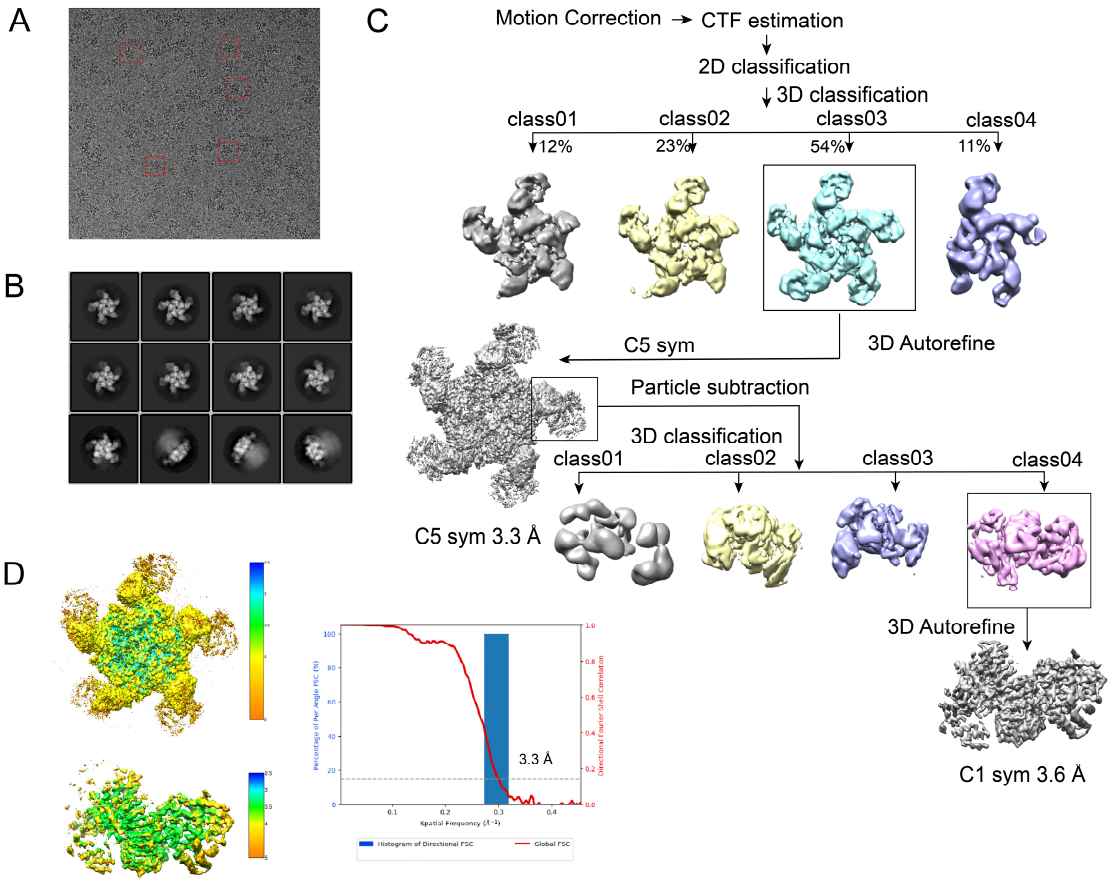

Fig. S2. 3D reconstruction of the Sr35 resistosome induced by wild-type AvrSr35. (**A**) Representative electron micrograph of Sr35 resistosome embedded in vitreous ice. (**B**) Representative views of 2D class averages. (**C**) Flowchart of Cryo-EM data processing and 3D reconstruction of the Sr35 resistosome. (**D**) Local resolution map calculated using Relion for Sr35 resistosome (top) and subtraction part (bottom). Right panel: FSC curves at 0.143 of the final reconstruction of the Sr35 resistosome.

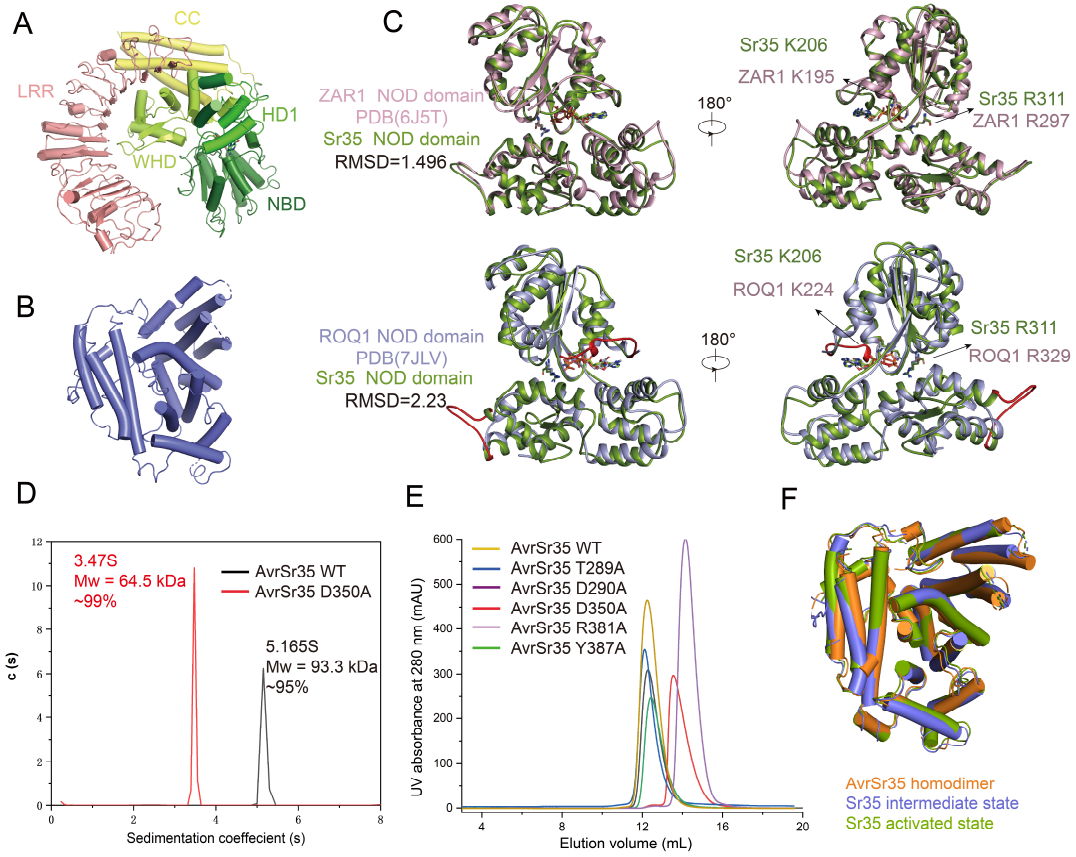

Fig. S3. Structures of Sr35 and AvrSr35 in active Sr35 complex. (**A**) The cartoon representation of Sr35 in Sr35 resistosome structure. CC, yellow; NBD, WHD, and HD1, forest, TV green, and limon, respectively; LRR, salmon. (**B**) Cartoon representation of AvrSr35 in Sr35 resistosome structure. (**C**) Structural comparison between the NOD domains of Sr35 and its homologues ZAR1 (top) and ROQ1 (bottom) in oligomerized state. Since the Sr35 and ROQ1 resistosomes have different aggregation states, the Sr35 loops contacting neighboring protomer (indicated in red) have different spatial conformations compared to their counterparts in ROQ1 NOD domain. Key amino acid residues involved in (d)ATP binding are labeled and RMSD values are indicated. (**D**) Analytical ultracentrifugation (AUC) assay of the AvrSr35 and AvrSr35^{D350A}. (**E**) Gel filtration chromatograms of wild-type AvrSr35 and its mutant variants. Please note that the elution volumes of AvrSr35 mutans R381A and D350A are significantly increased. (**F**) Structural alignment of AvrSr35 from

homodimer (orange) and Sr35-bound AvrSr35 (from intermediated state and activated state) (green and slate) showed a high similarity with a root mean square deviation (RMSD) value of 1.067 Å and 1.277 Å respectively.

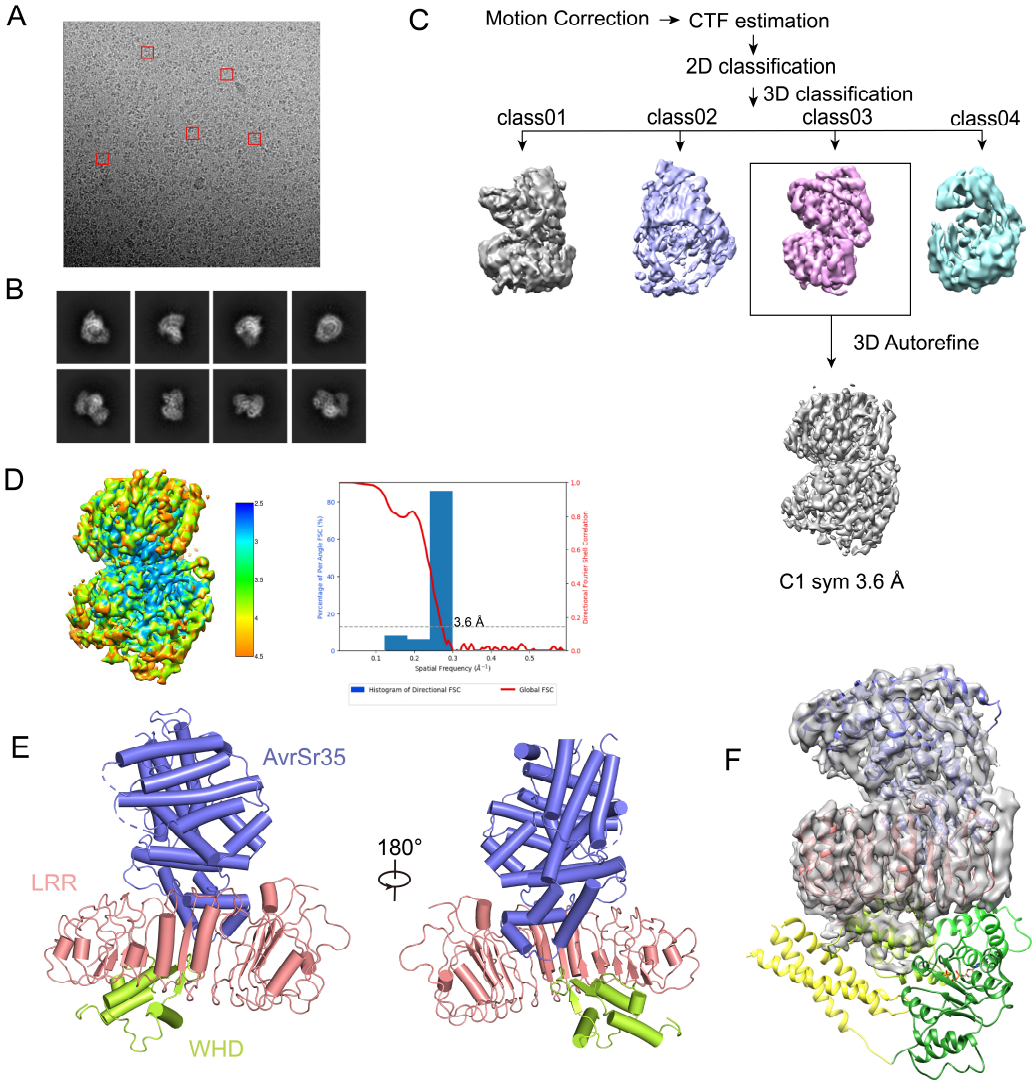

Fig. S4. 3D reconstruction of Sr35 and AvrSr35 complex. (**A**) Representative electron micrograph of Sr35-AvrSr35 complex embedded in vitreous ice. (**B**) Representative views of 2D class averages. (**C**) Flowchart of cryo-EM data processing and 3D reconstruction of the Sr35-AvrSr35 complex. (**D**) Local resolution map for the Sr35-AvrSr35 complex calculated using cryoSPARC. Right panel: FSC curves at 0.143 of the final reconstruction of the Sr35-AvrSr35 complex. (**E**) Overall structure of binary complex of Sr35 and AvrSr35. (**F**) The fitting of Sr35 resistosome protomer model into cryo-EM map of Sr35-AvrSr35 complex. The domains of Sr35 are

shown in different colors: CC, yellow; NBD, WHD, and HD1, forest, TV green, and limon, respectively; LRR, salmon. AvrSr35 is colored slate.

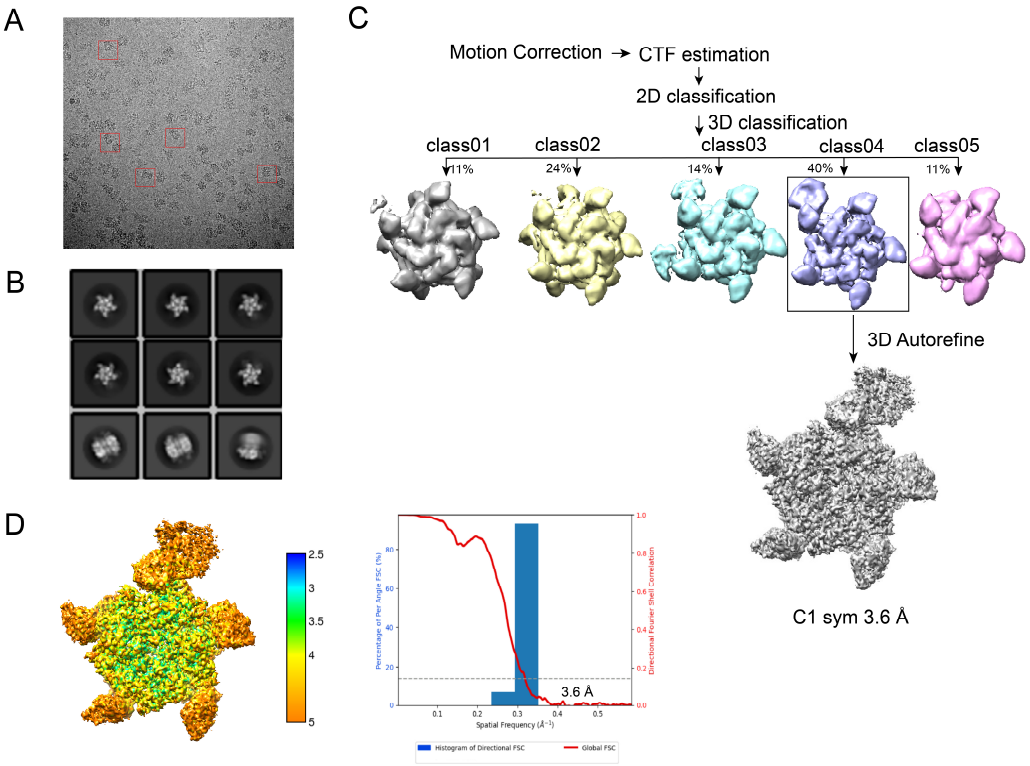

Fig. S5. 3D reconstruction of the SUMO-tagged Sr35 resistosome induced by AvrSr35^{R381A}.

(**A**) Representative electron micrograph of AvrSr35^{R381A} induced SUMO-Sr35 resistosome embedded in vitreous ice. (**B**) Representative views of 2D class averages. (**C**) Flowchart of Cryo-EM data processing and 3D reconstruction of the AvrSr35^{R381A} induced SUMO-Sr35 resistosome. (**D**) Local resolution map calculated using Relion for AvrSr35^{R381A} induced Sr35 resistosome. Right panel: FSC curves at 0.143 of the final reconstruction of the Sr35 resistosome.

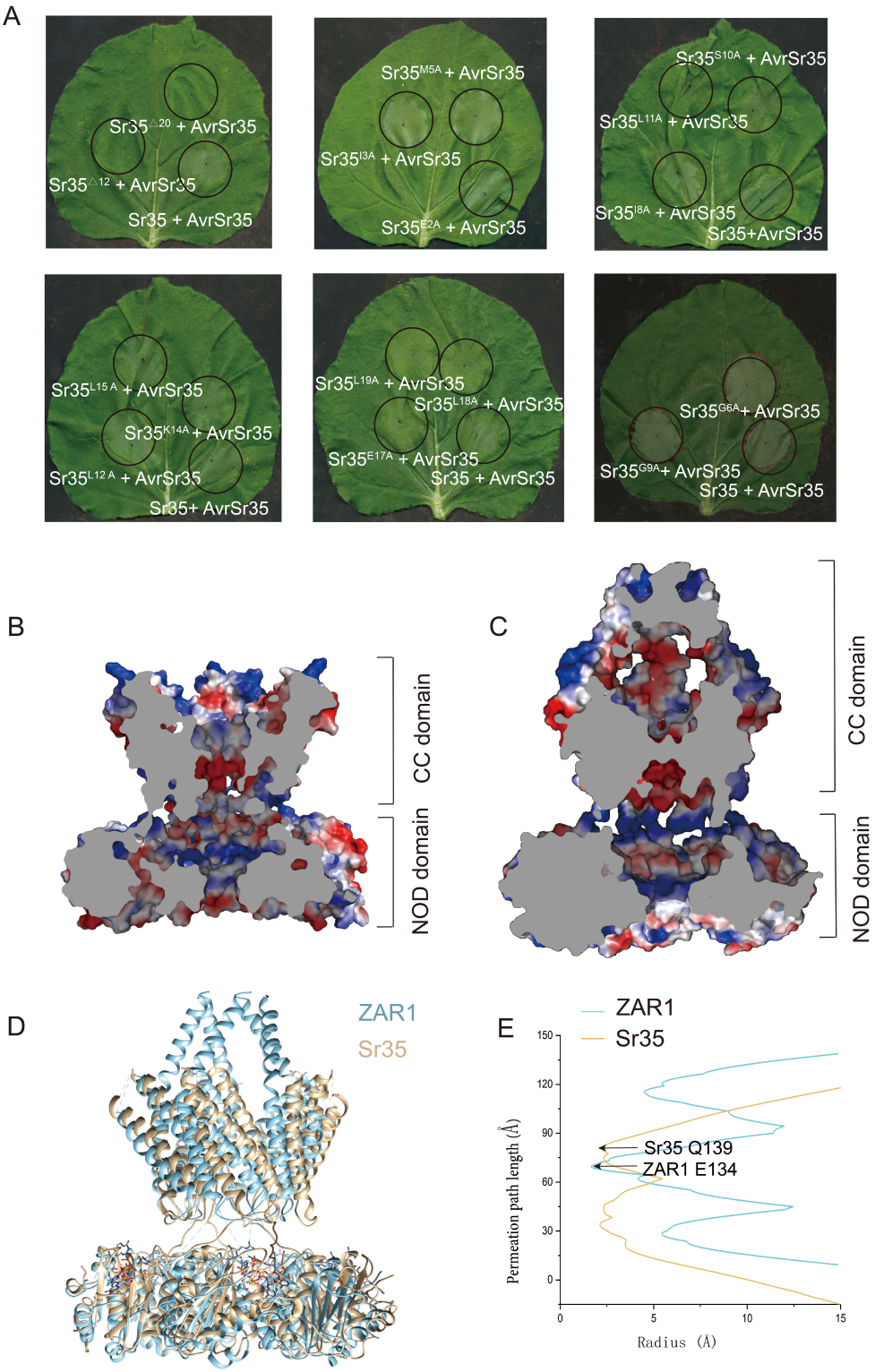

Fig. S6. The predicted very N-terminal helix is indispensable for Sr35-mediated immune signaling and cell death. (**A**) Co-infiltration of tobacco leaves with wild-type or mutant variants of Sr35 and AvrSr35 constructs. The images were taken 36–48 hpi. The experiment was performed

three times. (**B**) and (**C**) Cross-sections of central pores in Sr35 and ZAR1 resistosomes with the electrostatic potential shown on the external surface of the molecular envelope. (**D**) Superimposition of pore-forming domains (including CC, NBD, and HD1 domain) of Sr35 and ZAR1 (PDB: 6J5T). (**E**) Plot depicting the pore radius as a function of the pore axis. The central cavity and intracellular cavity are indicated.

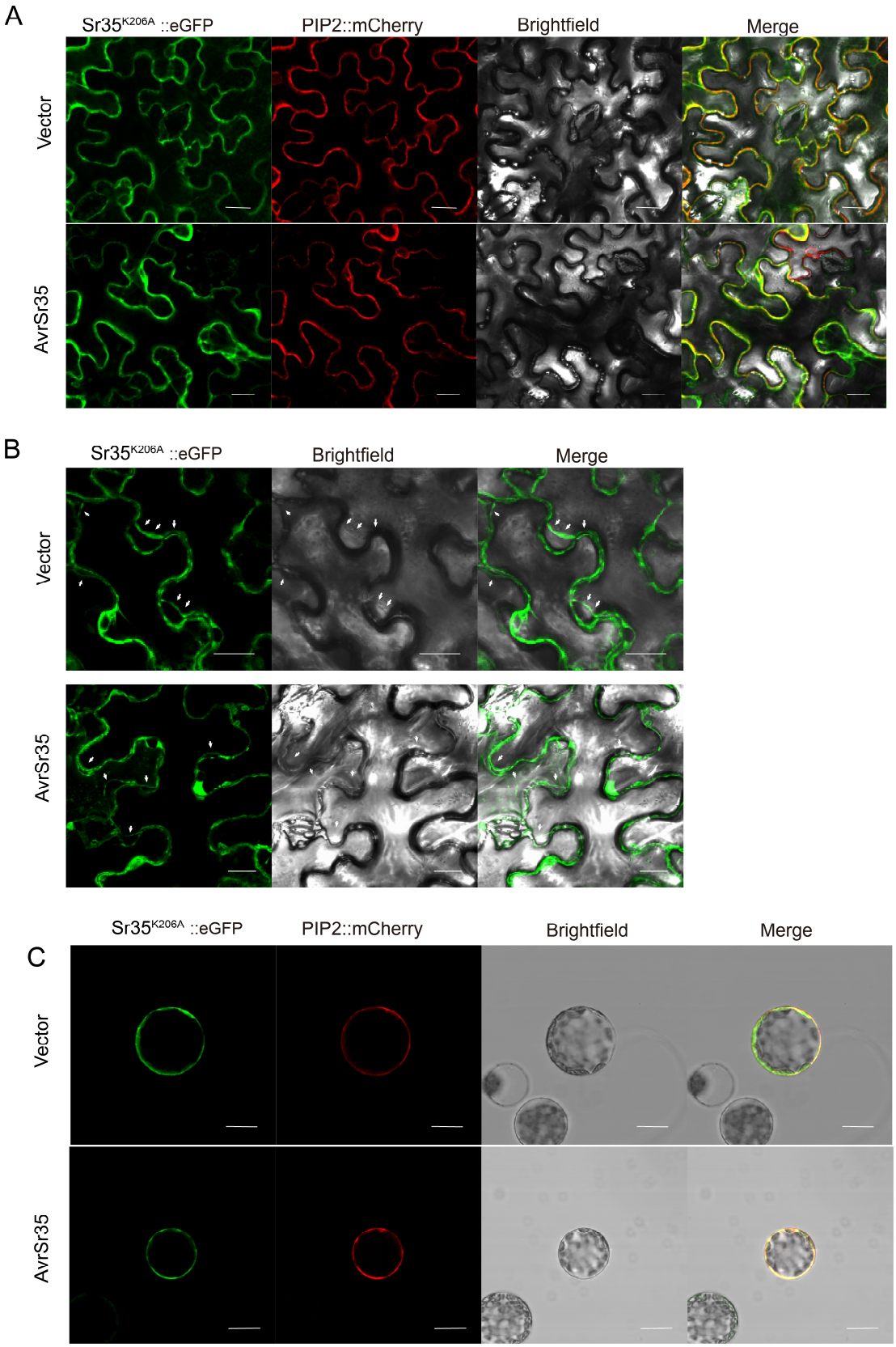

Fig. S7. Subcellular localization of Sr35^{K206A}. (**A**) Localization of eGFP-tagged Sr35^{K206A} (Sr35^{K206A}::eGFP) in *N. benthamiana* in the absence or presence of AvrSr35. (**B**) Subcellular

localization of Sr35^{K206A}::eGFP in *N. benthamiana* in the absence or presence of AvrSr35 after plasmolysis. Retracted PM is indicated by white arrows. (**C**) Subcellular localization of Sr35^{K206A}::eGFP in protoplasts in the absence or presence of AvrSr35. Cell membranes were traced using mCherry-tagged PIP2 (PIP2::mCherry). Scale bar: 20 μM.

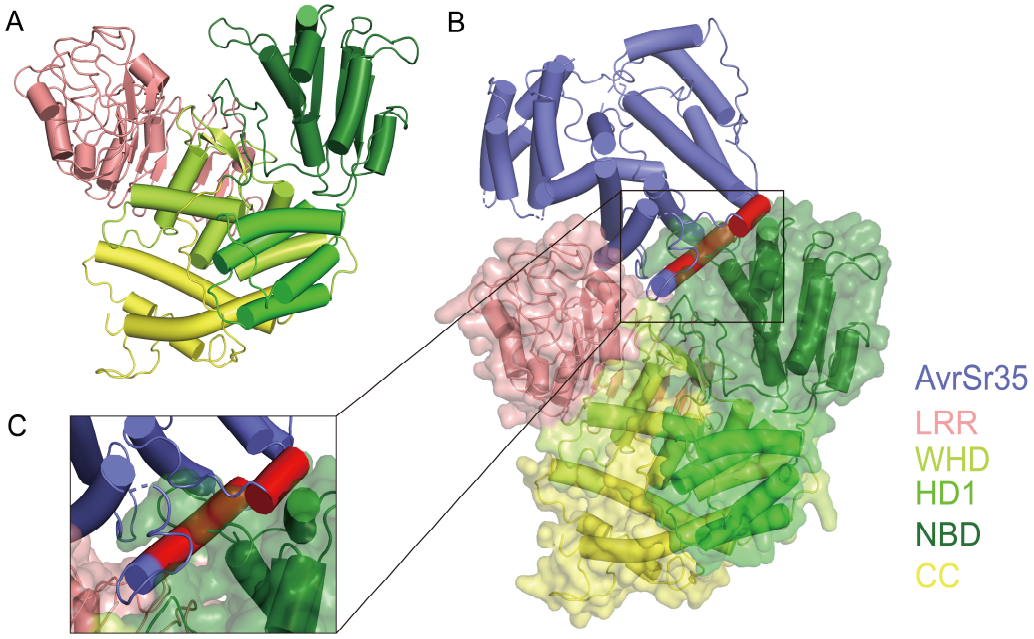

Fig. S8. Steric hindrance between AvrSr35 and Sr35^{NOD} upon Sr35 activation. (**A**) Modeled structure of inactive Sr35. (**B**) Structural alignment of the modeled inactive Sr35 with AvrSr35-bound Sr35. (**C**) The steric clash between inactive Sr35 and AvrSr35 which is shown in red. The domains and subdomains of Sr35 are shown in different colors: CC, yellow; NBD, WHD, and HD1, forest, TV green, and limon, respectively; LRR, salmon. AvrSr35 is colored slate.

Table S1. Cryo-EM statistics and model refinement for the Sr35 resistosome

Data collection	**Sr35 resistosome**	**AvrSr35^{R381A} induced SUMO- Sr35 resistosome**	**Sr35-AvrSr35 complex**
Cryo-electron microscope voltage (kV)	300	300	300
Detector	Gatan K3 Summit	Gatan K3 Summit	Gatan K2 Summit
Energy filter silt width (eV)	20	20	8
Magnification	81,000×	81,000 ×	165,000 ×
Pixel size (Å)	1.09	1.09	0.84
Total electron exposure ($e^-/Å^2$)	50	50	50
Number of frames collected	32	32	32
Defocus range (μm)	-1.0~-1.6	-1.0~-1.6	-1.2~-1.8
Automation software	EPU	EPU	SeriEM
3D reconstruction			
Software	Relion	Relion	Relion; cryoSPARC
Total number particles for final refinement	54000	30530	85070
Symmetry imposed	C5	C1	C1
Resolution range (Å)	3.0-4.0	3.5-4.5	3.0-4.0
Resolution (Å) after refinement (FSC=0.143)	3.3	3.6	3.6
Map sharpening B-factor ($Å^2$)	-100	-50	-85
Refinement and validation			
Software	phenix.real_space_refine	phenix.real_space_refine	phenix.real_space_refine
Model resolution (Å)	3.3	3.6	3.6
Model composition			
Non-hydrogen atoms	49700	36448	6444
Protein residues	6160	4529	795
Map-model CC (overall/local)	0.76	0.82	0.78
B factors ($Å^2$)			
R.M.S deviations			
Bonds lengths (Å)	0.003	0.005	0.004
Bonds angles (°)	0.641	0.797	0.727
MolProbity score	2.09	2.24	2.02

Table S1. Cont.

Data collection	Sr35 resistosome	AvrSr35R381A induced SUMO- Sr35 resistosome	Sr35-AvrSr35 complex
Clash score	12.11	15.06	12.75
Rotamer outliers (%)	0.05	0.00	0.28
Cβ outliers (%)	0	0.00	0.00
CaBLAM outliers (%)	4.93	5.39	3.26
EMRinger score			
Ramachandran plot (%)			
Favored region	91.89	89.82	93.98
Allowed region	8.09	10.18	5.89
Outlier region	0.02	0.00	0.13

Table S2. Data collection and optimization information of X-ray crystal structure of AvrSr35

Dataset	SeMet-AvrSr35
Data collection	
Beamline	SSRF BL19-U1
Wavelength (Å)	0.9792
Space group	$P2_12_12_1$
Cell dimensions	
a, b, c (Å)	54.12, 115.273, 143.162
α, β, γ (°)	90.00, 90.00, 90.00
Resolution range (Å)	44.89-2.06 (2.134-2.06)
Completeness (%)	97.71 (98.59)
Average *I*/sigma (*I*)	19 (11.7)
R_{merge}	0.142 (0.316)
Multiplicity	26.3 (5.4)
Refinement	
Resolution (Å)	2.06
No. reflections	55013 (5445)
R_{work}/R_{free} (%)	24.42 (30.37)/27.37 (32.99)
No. atoms	
Protein	743
Solvent	57
Average *B*-factors (Å^2)	32.25
R.m.s deviations	
Bond lengths (Å)	0.014
Bond angles (°)	1.66
Ramachandran plot (%)	
Favored region	98.20
Allowed region	1.80
Outliers region	0.1557

*Highest resolution shell is shown in parentheses.

Table S3. Buried surface area of the AvrSr35 dimerization surface and AvrSr35-Sr35 complex

	AvrSr35 dimer		AvrSr35-Sr35 complex	
	AvrSr35-1	**AvrSr35-2**	**AvrSr35**	**Sr35**
Number of residues				
interface	23	21	30	37
surface	347	343	393	821
total	375	368	394	838
Solvent-accessible area, Å²				
interface	716.5	713.7	1206.2	1165.5
total	18068.5	17640.3	21210.9	43071.9
Solvation energy, kcal/mol				
isolated structure	-339.2	-332.1	361.1	-824.6
gain on complex formation	-2.4	-0.9	0.9	-0.9
average gain	-1.8	-1.7	-2.9	-3.2
P-value	0.422	0.633	0.877	0.745
Buried surface area, Å²	1430.2		2371.7	

*Interface areas were calculated using PISA (https://www.ebi.ac.uk/pdbe/pisa/)

Table S4. Primers used in this study

Primer name	Primer sequence 5'-3'
Sr35 BP F	AAAAAGCAGGCTTCATGGAGATTGCCATGGGG
Sr35 BP R	AGAAAGCTGGGTCCCATATATCGAGGATGGGACG
Sr35 BamH1 F	CGCGGATCCATGGAGATTGCCATGGGG
Sr35 Xho1 R	CCGCTCGAGTTATCACCATATATCGAGGATGG
$Sr35^{\Delta 12}$ BamH1 F	CGCGGATCCCCGAAGCTCGGCGAGCTGCTCATC
$Sr35^{\Delta 20}$ BamH1 F	CGCGGATCCGGCGAGATCACCCTGGAGAAAAAAG
$Sr35^{\Delta 12}$ BP F	AAAAAGCAGGCTTCCCGAAGCTCGGCGAGC
$Sr35^{\Delta 20}$ BP F	AAAAAGCAGGCTTCGGCGAGATCACCCTGGAG
AvrSr35 △SP BamH1 F	CGCGGATCCATGGTACAAATAGATGACCGAAAGGC
AvrSr35 △SP Xho1 R	CCGCTCGAGTTACAATTTGCCTTCATGAACATTGG
AvrSr35 △SP LIC F	TACTTCCAATCCAATGCCATGAGGAACTTTGCTGCAGATAGA
AvrSr35 △SP LIC R	TTATCCACTTCCAATGTTACAATTTGCCTTCATGAACATTGG
AvrSr35 C-stop △SP BP F	AAAAAGCAGGCTTC ATGAGGAACTTTGCTGCAGATAGAGTC
AvrSr35 C-stop △SP BP R	AGAAAGCTGGGTCCAATTTGCCTTCATGAACATTGGATG
$Sr35^{Q139A}$ F	GCTGCGTGCGAGGTACGAGCAAGAGATGCGGGACACTAG
$Sr35^{Q139A}$ R	GTACCTCGCACGCAGCTCGGCCAACTGCTTTGCTTGAAG
$Sr35^{Y141A}$ F	TCAGAGGGCCGAGCAAGAGATGCGGGACACTA
$Sr35^{Y141A}$ R	CTTGCTCGGCCCTCTGACGCAGCTCGGCCAAC
$Sr35^{R157A}$ F	ACCCTGCCATGATGGCCTTGTACACAGATGTGACA
$Sr35^{R157A}$ R	CATCATGGCAGGGTCAACACTAGTATTAGCACTA
$Sr35^{K206A}$ F	GTTAGGCGCGACGACTCTTGCCAAAGCAGCATACG
$Sr35^{K206A}$ R	GAGTCGTCGCGCCTAACCCACCAAATCCAACAAT
$Sr35^{R311A}$ F	CAACCGCAAATGTTAGTGTCTCTGAAGCATGTTGC
$Sr35^{R311A}$ R	AACATTTGCGGTTGTCGTGATTAGTCGGCTTCCGG
$Sr35^{Y654A}$ F	TTGATGCTGGTATGAAGCTGCCATCTGGGATAGGC
$Sr35^{Y654A}$ R	CATACCAGCATCAACATACAGGCACATTAGACGTCTTAG
$Sr35^{D673A}$ F	TAGATGCCCTGGGGTTATCTGACGTGGACCTTGATTT
$Sr35^{D673A}$ R	CCAGGGCATCTAGCACTTCTAGGAAAGTCAGGTTGC
$Sr35^{R730A}$ F	TCAATGCTGGACTCATCAATTGCTTGAGCGAACATT
$Sr35^{R730A}$ R	GTCCAGCATTGACAAATACATCTAGACTGTCCAG
$Sr35^{R755A}$ F	TCAAAAGCAAGTTGGTTCAAGACATTGCCGTCATGGATT
$Sr35^{R755A}$ R	CAACTTGCTTTTGACGGGAAAGCCAATCTACAGAG
$Sr35^{E809A}$ F	GTGTTCGCAGAAGCGCATGAGGTGGAAGCGCCCGTCC
$Sr35^{E809A}$ R	GCTTCTGCGAACACAGAATAATTCCATATCTCAAG
$Sr35^{R854H/W856R/T858S}$ F	CCAAGGCTTAAACATCTTAGGTTCAGCTTCCCA
$Sr35^{R854H/W856R/T858S}$ R	CACTTGGCTGGGAAGCTGAACCTAAGATGTTTAAG
$Sr35^{E2A}$ F	ATGGCGATTGCCATGGGGGCTATC
$Sr35^{E2A}$ R	GGCAATCGCCATGAAGCCTGCTTTTT
$Sr35^{I3A}$ F	ATGGAGGCTGCCATGGGGGCTATCG
$Sr35^{I3A}$ R	GGCAGCCTCCATGAAGCCTGCTTTT
$Sr35^{M5A}$ F	ATTGCCGCGGGGGCTATCGGCTCTC
$Sr35^{M5A}$ R	CCCCCGCGGCAATCTCCATGAAGCC

Table S4. Cont.

Primer name	Primer sequence 5'-3'
$Sr35^{G6A}$ R	GCTTCGGGAGGAGAGAGCCGATAGCCGCCATGGCAATCTCCAT
$Sr35^{I8A}$ F	GGGCTGCCGGCTCTCTCCTCCCGAA
$Sr35^{I8A}$ R	GAGCCGGCAGCCCCCATGGCAATCT
$Sr35^{G9A}$ F	TTGCCATGGGGGCTATCGCCTCTCTCCTCCCG
$Sr35^{G9A}$ R	CGGGAGGAGAGAGGCGATAGCCCCCATGGCAA
$Sr35^{S10A}$ F	TATCGGCGCTCTCCTCCCGAAGCTCG
$Sr35^{S10A}$ R	GAGGAGAGCGCCGATAGCCCCCATG
$Sr35^{L11A}$ F	GGCTCTGCCCTCCCGAAGCTCGGCGA
$Sr35^{L11A}$ R	CGGGAGGGCAGAGCCGATAGCCCCCA
$Sr35^{L12A}$ F	CTCTCGCCCCGAAGCTCGGCGAGCTG
$Sr35^{L12A}$ R	CTTCGGGGCGAGAGAGCCGATAGCC
$Sr35^{K14A}$ F	CTCCCGGCGCTCGGCGAGCTGCTCAT
$Sr35^{K14A}$ R	CCGAGCGCCGGGAGGAGAGAGCCGA
$Sr35^{L15A}$ F	CCGAAGGCCGGCGAGCTGCTCATCGG
$Sr35^{L15A}$ R	TCGCCGGCCTTCGGGAGGAGAGAGCC
$Sr35^{E17A}$ F	TCGGCGCGCTGCTCATCGGCGAGATC
$Sr35^{E17A}$ R	AGCAGCGCGCCGAGCTTCGGGAGGAG
$Sr35^{L18A}$ F	GCGAGGCGCTCATCGGCGAGATCACC
$Sr35^{L18A}$ R	CGATGAGCGCCTCGCCGAGCTTCGGG
$Sr35^{L19A}$ F	GAGCTGGCCATCGGCGAGATCACCCT
$Sr35^{L19A}$ R	GCCGATGGCCAGCTCGCCGAGCTTCG
$AvrSr35^{D291A}$ △SP F	GAAGTTGATCACAGAGGCTGAGATGCTAAAAATTC
$AvrSr35^{D291A}$ △SP R	GAATTTTTAGCATCTCAGCCTCTGTGATCAACTTC
$AvrSr35^{D350A}$ △SP F	AAAAAATAAAGCAAGTGCTTCAAGCTATCTTGGATG
$AvrSr35^{D350A}$ △SP R	CATCCAAGATAGCTTGAAGCACTTGCTTTATTTTTT
$AvrSr35^{D379A}$ △SP F	GAAAGGAGTATGTTTTTCCAAGCTGGAAGAAAATATGCTGAATTG
$AvrSr35^{D379A}$ △SP R	CAATTCAGCATATTTTCTTCCAGCTTGGAAAAACATACTCCTTTC
$AvrSr35^{D379A/G380A}$ △SP F	GAAAGGAGTATGTTTTTCCAAGCTGCAAGAAAATATGCTGAATTG
$AvrSr35^{D379A/G380A}$ △SP R	CAATTCAGCATATTTTCTTGCAGCTTGGAAAAACATACTCCTTTC
$AvrSr35^{R381A}$ △SP F	ATGTTTTTCCAAGATGGAGCAAAATATGCTGAAT
$AvrSr35^{R381A}$ △SP R	ATTCAGCATATTTTGCTCCATCTTGGAAAAACAT
$AvrSr35^{Y383A}$ △SP F	TTTTCCAAGATGGAAGAAAAGCTGCTGAATTGTATGCATT
$AvrSr35^{Y383A}$ △SP R	AATGCATACAATTCAGCAGCTTTTCTTCCATCTTGGAAAA
$AvrSr35^{Y387A}$ △SP F	AGAAAATATGCTGAATTGGCTGCATTTTCTAAAAGTCCC
$AvrSr35^{Y387A}$ △SP R	GGGACTTTTAGAAAATGCAGCCAATTCAGCATATTTTCT
$AvrSr35^{E401A}$ △SP F	GGGGCGCACCTCAAAGATCTGTTAGCTAAAATC
$AvrSr35^{E401A}$ △SP R	AGGTGCGCCCCAGGTATTATTTTCCTGTGGGGAC

Table S5. Plasmids generated in this study for protein expression and pull-down assay.

Construct	Plasmid	Primers	Template	Cloning method
SUMO-Sr35	pFastBac 1	Sr35 BamH1 F, Sr35 Xho1 R	pET28a-Sr35 (synthetic gene)	double digestion-ligation cloning
SUMO-Sr35$^{\Delta 12}$	pFastBac 1	Sr35$^{\triangle 12}$ BamH1 F, Sr35 Xho1 R	pET28a-Sr35 (synthetic gene)	double digestion-ligation cloning
SUMO-Sr35$^{\Delta 20}$	pFastBac 1	Sr35$^{\triangle 20}$ BamH1 F, Sr35 Xho1 R	pET28a-Sr35 (synthetic gene)	double digestion-ligation cloning
SUMO-Sr35^{Q139A}	pFastBac 1	Sr35^{Q139A} F, Sr35^{Q139A} R	pFastBac 1-SUMO-Sr35	double digestion-ligation cloning
SUMO-Sr35^{Y141A}	pFastBac 1	Sr35^{Y141A} F, Sr35^{Y141A} R	pFastBac 1-SUMO-Sr35	double digestion-ligation cloning
SUMO-Sr35^{R157A}	pFastBac 1	Sr35^{R157A} F, Sr35^{R157A} R	pFastBac 1-SUMO-Sr35	double digestion-ligation cloning
SUMO-Sr35^{K206A}	pFastBac 1	Sr35^{K206A} F, Sr35^{K206A} R	pFastBac 1-SUMO-Sr35	double digestion-ligation cloning
SUMO-Sr35 ^{R311A}	pFastBac 1	Sr35 ^{R311A} F, Sr35 ^{R311A} R	pFastBac 1-SUMO-Sr35	double digestion-ligation cloning
SUMO-Sr35^{Y654A}	pFastBac 1	Sr35^{Y654A} F, Sr35^{Y654A} R	pFastBac 1-SUMO-Sr35	double digestion-ligation cloning
SUMO-Sr35^{D673A}	pFastBac 1	Sr35^{D673A} F, Sr35^{D673A} R	pFastBac 1-SUMO-Sr35	double digestion-ligation cloning
SUMO-Sr35^{R730A}	pFastBac 1	Sr35^{R730A} F, Sr35^{R730A} R	pFastBac 1-SUMO-Sr35	double digestion-ligation cloning
SUMO-Sr35^{R755A}	pFastBac 1	Sr35^{R755A} F, Sr35^{R755A} R	pFastBac 1-SUMO-Sr35	double digestion-ligation cloning
SUMO-Sr35$^{R730A/R755A}$	pFastBac 1	Sr35^{R730A} F, Sr35^{R730A} R, Sr35^{R755A} F, Sr35^{R755A} R	pFastBac 1-SUMO-Sr35, pFastBac 1-SUMO-Sr35^{R730A}	double digestion-ligation cloning
SUMO-Sr35^{E809A}	pFastBac 1	Sr35^{E809A} F, Sr35^{E809A} R	pFastBac 1-SUMO-Sr35	double digestion-ligation cloning
SUMO-Sr35$^{R854H/W856R/T858S}$	pFastBac 1	Sr35$^{R854H/W856R/T858S}$ F, Sr35$^{R854H/W856R/T858S}$ R	pFastBac 1-SUMO-Sr35	double digestion-ligation cloning
AvrSr35 △SP	pMCSG7	AvrSr35 △SP LIC F, AvrSr35 △SP LIC R	pET28a-AvrSr35 (synthetic gene)	ligation-independent cloning (LIC)
AvrSr35^{D291A} △SP	pMCSG7	AvrSr35^{D291A} △SP F, AvrSr35^{D291A} △SP R	pMCSG7 -AvrSr35 △SP	ligation-independent cloning (LIC)
AvrSr35^{D350A} △SP	pMCSG7	AvrSr35^{D350A} △SP F, AvrSr35^{D350A} △SP R	pMCSG7 -AvrSr35 △SP	ligation-independent cloning (LIC)

Table S5. Cont.

Construct	Plasmid	Primers	Template	Cloning method
AvrSr35^{D379A} △SP	pMCSG7	AvrSr35^{D379A}△SP F, AvrSr35^{D379A} △SP R	pMCSG7 -AvrSr35 △SP	ligation-independent cloning (LIC)
AvrSr35$^{D379A/G380A}$ △SP	pMCSG7	AvrSr35$^{D379A/G380A}$ △SP F, AvrSr35$^{D379A/G380A}$ △SP R	pMCSG7 -AvrSr35 △SP	ligation-independent cloning (LIC)
AvrSr35^{R381A} △SP	pMCSG7	AvrSr35^{R381A} △SP F, AvrSr35^{R381A} △SP R	pMCSG7 -AvrSr35 △SP	ligation-independent cloning (LIC)
AvrSr35^{Y383A} △SP	pMCSG7	AvrSr35^{Y383A} △SP F, AvrSr35^{Y383A} △SP R	pMCSG7 -AvrSr35 △SP	ligation-independent cloning (LIC)
AvrSr35^{Y387A} △SP	pMCSG7	AvrSr35^{Y387A} △SP F, AvrSr35^{Y387A} △SP R	pMCSG7 -AvrSr35 △SP	ligation-independent cloning (LIC)
AvrSr35^{E401A} △SP	pMCSG7	AvrSr35^{E401A} △SP F, AvrSr35^{E401A} △SP R	pMCSG7 -AvrSr35 △SP	ligation-independent cloning (LIC)
GST-AvrSr35 △SP	pGEX-6P-1	AvrSr35 △SP BamH1 F, AvrSr35 △SP Xho1 R	pET28a-AvrSr35 (synthetic gene)	double digestion-ligation cloning
GST-AvrSr35^{D291A} △SP	pGEX-6P-1	AvrSr35^{D291A} △SP F, AvrSr35^{D291A} △SP R	pGEX-6P-1-AvrSr35 △SP	double digestion-ligation cloning
GST-AvrSr35^{D350A} △SP	pGEX-6P-1	AvrSr35^{D350A} △SP F, AvrSr35^{D350A} △SP R	pGEX-6P-1-AvrSr35 △SP	double digestion-ligation cloning
GST-AvrSr35^{R381A} △SP	pGEX-6P-1	AvrSr35^{R381A} △SP F, AvrSr35^{R381A} △SP R	pGEX-6P-1-AvrSr35 △SP	double digestion-ligation cloning
GST-AvrSr35^{Y387A} △SP	pGEX-6P-1	AvrSr35^{Y387A} △SP F, AvrSr35^{Y387A} △SP R	pGEX-6P-1-AvrSr35 △SP	double digestion-ligation cloning

Table S6. Plasmids generated in this study for entry clones for *N. benthamiana* assays.

Construct	Plasmid	Primers	Template	Cloning method
Sr35	pDONR207	Sr35 BP F, Sr35 BP R	pET28a-Sr35 (synthetic gene)	BP Gateway
$Sr35^{\Delta 12}$	pDONR207	$Sr35^{\Delta 12}$ BP F, Sr35 BP R	pET28a-Sr35 (synthetic gene)	BP Gateway
$Sr35^{\Delta 20}$	pDONR207	$Sr35^{\Delta 20}$ BP F, Sr35 BP R	pET28a-Sr35 (synthetic gene)	BP Gateway
$Sr35^{Q139A}$	pDONR207	$Sr35^{Q139A}$ F, $Sr35^{Q139A}$ R	pDONR207-Sr35	BP Gateway
$Sr35^{Y141A}$	pDONR207	$Sr35^{Y141A}$ F, $Sr35^{Y141A}$ R	pDONR207-Sr35	BP Gateway
$Sr35^{R157A}$	pDONR207	$Sr35^{R157A}$ F, $Sr35^{R157A}$ R	pDONR207-Sr35	BP Gateway
$Sr35^{K206A}$	pDONR207	$Sr35^{K206A}$ F, $Sr35^{K206A}$ R	pDONR207-Sr35	BP Gateway
$Sr35^{R311A}$	pDONR207	$Sr35^{R311A}$ F, $Sr35^{R311A}$ R	pDONR207-Sr35	BP Gateway
$Sr35^{Y654A}$	pDONR207	$Sr35^{Y654A}$ F, $Sr35^{Y654A}$ R	pDONR207-Sr35	BP Gateway
$Sr35^{D673A}$	pDONR207	$Sr35^{D673A}$ F, $Sr35^{D673A}$ R	pDONR207-Sr35	BP Gateway
$Sr35^{R730A}$	pDONR207	$Sr35^{R730A}$ F, $Sr35^{R730A}$ R	pDONR207-Sr35	BP Gateway
$Sr35^{R755A}$	pDONR207	$Sr35^{R755A}$ F, $Sr35^{R755A}$ R	pDONR207-Sr35	BP Gateway
$Sr35^{R730A/R755A}$	pDONR207	$Sr35^{R730A}$ F, $Sr35^{R730A}$ R, $Sr35^{R755A}$ F, $Sr35^{R755A}$ R	pDONR207-Sr35, pDONR207-$Sr35^{R730A}$	BP Gateway
$Sr35^{E809A}$	pDONR207	$Sr35^{E809A}$ F, $Sr35^{E809A}$ R	pDONR207-Sr35	BP Gateway
$Sr35^{R854H/W856R/T858S}$	pDONR207	$Sr35^{R854H/W856R/T858S}$ F, $Sr35^{R854H/W856R/T858S}$ R	pDONR207-Sr35	BP Gateway
$Sr35^{E2A}$	pDONR207	$Sr35^{E2A}$ F, $Sr35^{E2A}$ R	pDONR207-Sr35	BP Gateway
$Sr35^{I3A}$	pDONR207	$Sr35^{I3A}$ F, $Sr35^{I3A}$ R	pDONR207-Sr35	BP Gateway
$Sr35^{M5A}$	pDONR207	$Sr35^{M5A}$ F, $Sr35^{M5A}$ R	pDONR207-Sr35	BP Gateway
$Sr35^{G6A}$	pDONR207	$Sr35^{G6A}$ F, $Sr35^{G6A}$ R	pDONR207-Sr35	BP Gateway
$Sr35^{I8A}$	pDONR207	$Sr35^{I8A}$ F, $Sr35^{I8A}$ R	pDONR207-Sr35	BP Gateway
$Sr35^{G9A}$	pDONR207	$Sr35^{G9A}$ F, $Sr35^{G9A}$ R	pDONR207-Sr35	BP Gateway
$Sr35^{S10A}$	pDONR207	$Sr35^{S10A}$ F, $Sr35^{S10A}$ R	pDONR207-Sr35	BP Gateway

Table S6. Cont.

Construct	Plasmid	Primers	Template	Cloning method
$Sr35^{L11A}$	pDONR207	$Sr35^{L11A}$ F, $Sr35^{L11A}$ R	pDONR207-Sr35	BP Gateway
$Sr35^{L12A}$	pDONR207	$Sr35^{L12A}$ F, $Sr35^{L12A}$ R	pDONR207-Sr35	BP Gateway
$Sr35^{K14A}$	pDONR207	$Sr35^{K14A}$ F, $Sr35^{K14A}$ R	pDONR207-Sr35	BP Gateway
$Sr35^{L15A}$	pDONR207	$Sr35^{L15A}$ F, $Sr35^{L15A}$ R	pDONR207-Sr35	BP Gateway
$Sr35^{E17A}$	pDONR207	$Sr35^{E17A}$ F, $Sr35^{E17A}$ R	pDONR207-Sr35	BP Gateway
$Sr35^{L18A}$	pDONR207	$Sr35^{L18A}$ F, $Sr35^{L18A}$ R	pDONR207-Sr35	BP Gateway
$Sr35^{L19A}$	pDONR207	$Sr35^{L19A}$ F, $Sr35^{L19A}$ R	pDONR207-Sr35	BP Gateway
AvrSr35 C-stop △SP	pDONR207	AvrSr35 C-stop △SP BP F, AvrSr35 C-stop △SP BP R	pET28a-AvrSr35 (synthetic gene)	BP Gateway
$AvrSr35^{D291A}$ △SP	pDONR207	$AvrSr35^{D291A}$ △SP F, $AvrSr35^{D291A}$ △SP R	pDONR207-AvrSr35	BP Gateway
$AvrSr35^{D350A}$ △SP	pDONR207	$AvrSr35^{D350A}$ △SP F, $AvrSr35^{D350A}$ △SP R	pDONR207-AvrSr35	BP Gateway
$AvrSr35^{D379A}$ △SP	pDONR207	$AvrSr35^{D379A}$△SP F, $AvrSr35^{D379A}$ △SP R	pDONR207-AvrSr35	BP Gateway
$AvrSr35^{D379A/G380A}$ △SP	pDONR207	$AvrSr35^{D379A/G380A}$ △SP F, $AvrSr35^{D379A/G380A}$ △SP R	pDONR207-AvrSr35	BP Gateway
$AvrSr35^{R381A}$ △SP	pDONR207	$AvrSr35^{R381A}$ △SP F, $AvrSr35^{R381A}$ △SP R	pDONR207-AvrSr35	BP Gateway
$AvrSr35^{Y383A}$ △SP	pDONR207	$AvrSr35^{Y383A}$ △SP F, $AvrSr35^{Y383A}$ △SP R	pDONR207-AvrSr35	BP Gateway

Table S6. Cont.

Construct	Plasmid	Primers	Template	Cloning method
AvrSr35^{Y387A} △SP	pDONR207	AvrSr35^{Y387A} △SP F, AvrSr35^{Y387A} △SP R	pDONR207-AvrSr35	BP Gateway
AvrSr35^{E401A} △SP	pDONR207	AvrSr35^{E401A} △SP F, AvrSr35^{E401A} △SP R	pDONR207-AvrSr35	BP Gateway
PIP2::mCherry C-stop	pDONR207	-	synthetic gene	BP Gateway

Table S7. Plasmids generated in this study. For cell-death assays, and confocal microscopy in *N. benthamiana*.

Construct	Plasmid	Primers	Template	Cloning method
Sr35::eGFP	pK7FWG2	-	pDONR207-Sr35	LR Gateway
$Sr35^{\Delta 12}$::eGFP	pK7FWG2	-	pDONR207-$Sr35^{\Delta 12}$	LR Gateway
$Sr35^{\Delta 20}$::eGFP	pK7FWG2	-	pDONR207-$Sr35^{\Delta 20}$	LR Gateway
$Sr35^{Q139A}$::eGFP	pK7FWG2	-	pDONR207-$Sr35^{Q139A}$	LR Gateway
$Sr35^{Y141A}$::eGFP	pK7FWG2	-	pDONR207-$Sr35^{Y141A}$	LR Gateway
$Sr35^{R157A}$::eGFP	pK7FWG2	-	pDONR207-$Sr35^{R157A}$	LR Gateway
$Sr35^{K206A}$::eGFP	pK7FWG2	-	pDONR207-$Sr35^{K206A}$	LR Gateway
$Sr35^{R311A}$::eGFP	pK7FWG2	-	pDONR207-$Sr35^{R311A}$	LR Gateway
$Sr35^{Y654A}$::eGFP	pK7FWG2	-	pDONR207-$Sr35^{Y654A}$	LR Gateway
$Sr35^{D673A}$::eGFP	pK7FWG2	-	pDONR207-$Sr35^{D673A}$	LR Gateway
$Sr35^{R730A}$::eGFP	pK7FWG2	-	pDONR207-$Sr35^{R730A}$	LR Gateway
$Sr35^{R755A}$::eGFP	pK7FWG2	-	pDONR207-$Sr35^{R755A}$	LR Gateway
$Sr35^{R730A/R755A}$::eGFP	pK7FWG2	-	pDONR207-$Sr35^{R730A/R755A}$	LR Gateway
$Sr35^{E809A}$::eGFP	pK7FWG2	-	pDONR207-$Sr35^{E809A}$	LR Gateway
$Sr35^{R854H/W856R/T858S}$::eGFP	pK7FWG2	-	pDONR207-$^{Sr35R854H/W856R/T858S}$	LR Gateway
$Sr35^{E2A}$::eGFP	pK7FWG2	-	pDONR207-$Sr35^{E2A}$	LR Gateway
$Sr35^{I3A}$::eGFP	pK7FWG2	-	pDONR207-$Sr35^{I3A}$	LR Gateway
$Sr35^{M5A}$::eGFP	pK7FWG2	-	pDONR207-$Sr35^{M5A}$	LR Gateway
$Sr35^{G6A}$::eGFP	pK7FWG2	-	pDONR207-$Sr35^{G6A}$	LR Gateway
$Sr35^{I8A}$::eGFP	pK7FWG2	-	pDONR207-$Sr35^{I8A}$	LR Gateway
$Sr35^{S10A}$::eGFP	pK7FWG2	-	pDONR207-$Sr35^{S10A}$	LR Gateway
$Sr35^{L11A}$::eGFP	pK7FWG2	-	pDONR207-$Sr35^{L11A}$	LR Gateway
$Sr35^{L12A}$::eGFP	pK7FWG2	-	pDONR207-$Sr35^{L12A}$	LR Gateway
$Sr35^{K14A}$::eGFP	pK7FWG2	-	pDONR207-$Sr35^{K14A}$	LR Gateway

Table S7. Cont.

Construct	Plasmid	Primers	Template	Cloning method
$Sr35^{L15A}$::eGFP	pK7FWG2	-	pDONR207-$Sr35^{L15A}$	LR Gateway
$Sr35^{E17A}$::eGFP	pK7FWG2	-	pDONR207-$Sr35^{E17A}$	LR Gateway
$Sr35^{L18A}$::eGFP	pK7FWG2	-	pDONR207-$Sr35^{L18A}$	LR Gateway
$Sr35^{L19A}$::eGFP	pK7FWG2	-	pDONR207-$Sr35^{L19A}$	LR Gateway
eGFP::AvrSr35 △SP	pK7WGF2	-	pDONR207-AvrSr35	LR Gateway
AvrSr35 △SP C-stop	pK7FWG2	-	pDONR207-AvrSr35	LR Gateway
eGFP::$AvrSr35^{D291A}$△SP	pK7WGF2	-	pDONR207-$AvrSr35^{D291A}$	LR Gateway
eGFP::$AvrSr35^{D350A}$ △SP	pK7WGF2	-	pDONR207-$AvrSr35^{D350A}$	LR Gateway
eGFP::$AvrSr35^{D379A}$ △SP	pK7WGF2	-	pDONR207-$AvrSr35^{D379A}$	LR Gateway
eGFP::$AvrSr35^{D379A/G380A}$ △SP	pK7WGF2	-	pDONR207-$AvrSr35^{D379A/G380A}$	LR Gateway
eGFP::$AvrSr35^{R381A}$ △SP	pK7WGF2	-	pDONR207-$AvrSr35^{R381A}$	LR Gateway
eGFP::$AvrSr35^{Y383A}$ △SP	pK7WGF2	-	pDONR207-$AvrSr35^{Y383A}$	LR Gateway
eGFP::$AvrSr35^{Y387A}$ △SP	pK7WGF2	-	pDONR207-$AvrSr35^{Y387A}$	LR Gateway
eGFP::$AvrSr35^{E401A}$ △SP	pK7WGF2	-	pDONR207-$AvrSr35^{E401A}$	LR Gateway
PIP::mCherry C-stop	pK7WGF2	-	pDONR207-PIP2;2-M-Cherry C-stop	LR Gateway

Table S8. Products used in this study.

Resource	Source	Identifier
Bacterial, cell and plant materials		
Escherichia coli Rosetta (DE3)	Weidi Biotechnology	CAT#: EC1010
Escherichia coli DH5α	Weidi Biotechnology	CAT#: DL1001
Escherichia coli DH10Bac	Weidi Biotechnology	CAT#: DL1071
Agrobacterium strain GV3101	Weidi Biotechnology	CAT#: AC1004
Spodoptera frugiperda 9 (Sf9) insect cells	Thermo Fisher	CAT#: A35243
Arabidopsis thaliana Col-0	provided by the Laboratory	-
Nicotiana benthamiana	provided by the Laboratory	-
Antibodies		
anti-GST antibody	Abcam	CAT#: ab138491
anti-His antibody	Abcam	CAT#: ab18184
Chemicals and reagents		
Cellfectin® Reagent	Thermo Fisher	CAT#: A38915
KOD-plus-neo	TOYOBO	CAT#: KOD-401
T4 DNA ligase	Thermo Fisher	CAT#: EL0014
T4 DNA polymerase	Thermo Fisher	CAT#: 18005025
BamH1	NEB	CAT#: R0136S
Xho1	NEB	CAT#: R0146S
SSP1	NEB	CAT#: R0132S
Dpn1	NEB	CAT#: R0176S
ATP	Sigma	CAT#: FLAAS
Gateway™ LR Clonase™	Thermo Fisher	CAT#: 11789013
Gateway™ BP Clonase™ II	Thermo Fisher	CAT#: 11789100
Essential Commercial Assays		
Plasmid mini kit	Omega	CAT#: D6943-02
Gel-Extraction Kit	Omega	CAT#: D2500-02